Tidal sand waves on the lower shoreface: effects on basin-scale hydrodynamics

L. Portos-Amill *University of Twente, Enschede, The Netherlands – l.portosamill@utwente.nl*
P.C. Roos *University of Twente, Enschede, The Netherlands – p.c.roos@utwente.nl*
J.H. Damveld *University of Twente, Enschede, The Netherlands – j.h.damveld@utwente.nl*
S.J.M.H. Hulscher *University of Twente, Enschede, The Netherlands – s.j.m.h.hulscher@utwente.nl*

ABSTRACT: Lower shoreface seabed dynamics are poorly understood. Tidal sand waves (as well as other bedforms) play an important role in the sediment transport and bed evolution of this region. Yet, they are usually overlooked in basin-scale modeling studies. The present work presents a novel method to parametrize bedform friction in order to include sand wave effects on the hydrodynamics of basin-scale domains (such as the North Sea, hundreds of km). Preliminary results show that, due to the presence of sand waves, the flow is deflected and modified in magnitude.

1 INTRODUCTION

The lower shoreface forms the transition between the inner shelf and the upper shoreface. It is usually covered by bedforms characterized by different spatial and temporal scales. We can find ripples (a few decimeters long), tidal sand waves (100 – 1000 m long), and ridges (5 – 10 km long). These bedforms are usually found to co-exist in the field, for example ripples on top of sand waves, and/or sand waves on top of ridges (van der Spek et al., 2022). Thus, they can interact and affect the flow through a modified bed roughness (Soulsby, 1983). As a result, they also affect sediment transport, and thus the morphodynamic evolution of the seabed, resulting in a closed hydro- and morphodynamic loop (Fig. 1).

However, sand waves as well as other bed patterns are mostly studied in isolation (e.g., Blondeaux, 1990; Hulscher, 1996; Roos et al., 2004). Little is known about the two-way

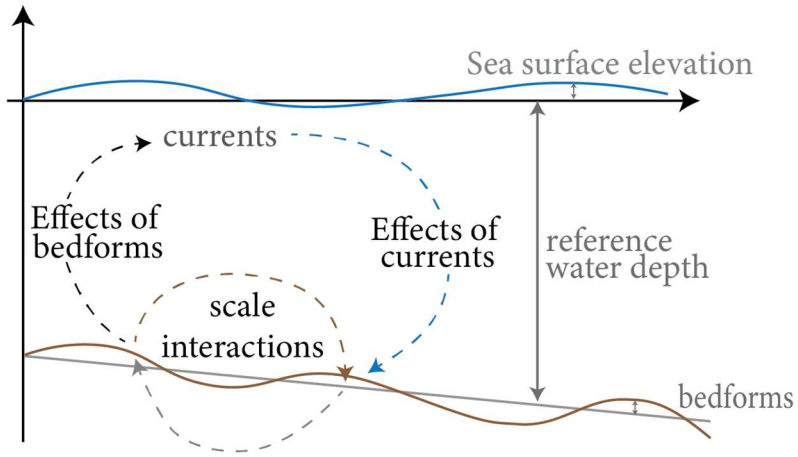

Figure 1. Sketch of the proposed research: We will investigate the effects of bedforms on the currents, but also the interactions between sand waves and larger-scale bedforms, which affect (and are affected by) the currents.

couplings between sand waves and other bedforms, and how these affect the flow. Consequently, the effects of bedforms on basin-scale flows (such as in the North Sea, see Fig. 2a) are usually not considered in modeling studies (see Brakenhoff et al., 2020, and references therein). Similarly, the effects of sand waves on the flow at a sand wave field scale (Fig. 2b) are poorly understood. The above mentioned knowledge gaps primarily concern the hydrodynamics of the lower shoreface. In addition, there is a lack of knowledge regarding the morphodynamics of sand waves on the lower shoreface. More specifically, the effects of a sloping background topography on sand wave evolution (Fig. 2c) and vice versa remain unclear. As part of the MELODY project (ModEling LOwer shoreface seabed DYnamics for a climate-proof coast), the proposed research will tackle these knowledge gaps in order to better understand the dynamics of sand waves on the lower shoreface. Since sand waves (as well as other bedforms) affect the flow and hence sediment transport, more insight on their dynamics will contribute to a better understanding and representation of the processes shaping the lower shoreface.

By addressing the above mentioned knowledge gaps, the proposed research aims to: (1) explain bedform effects on basin-scale hydrodynamics; (2) understand how sand waves affect the flow at sand wave field scales; and reveal sand wave morphodynamics superimposed on a sloping background topography (such as ridges or the lower shoreface) during (3) the sand wave formation stage, and (4) the subsequent evolution. Aims (1) and (2) will serve to better represent bedform-induced hydrodynamics on larger-scale domains (basin scale or sand wave field scale, respectively). Aims (3) and (4) will serve to gain system knowledge on sand wave dynamics on the lower shoreface.

This work focuses on the first aim, i.e., the effects of sand wave-induced friction on basin-scale hydrodynamics. An overview of the methodology used and preliminary results are presented and discussed in §2. Future research approaches are summarized in §3.

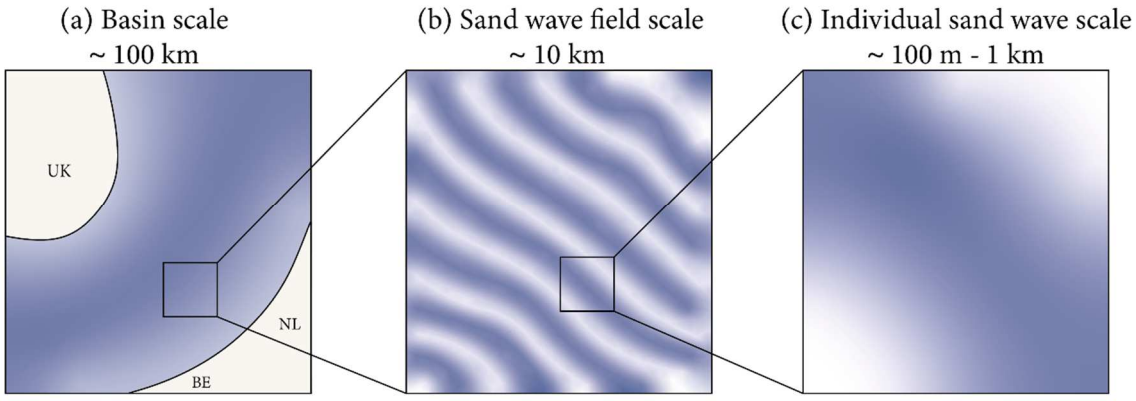

Figure 2. Sketch of the different spatial scales considered in the proposed research: (a) basin scale, such as the North Sea, corresponding to hundreds of km, (b) sand wave field scale, containing several sand waves within it, and corresponding to tens of km, and (c) individual sand wave scale, corresponding to hundreds of m. The proposed research aims to include sand wave effects on the hydrodynamics at basin (a) and sand wave field (b) scales, as well as understanding sand wave (c) morphodynamics superimposed on a sloping background topography.

2 BEDFORM-INDUCED FRICTION IN BASIN-SCALE FLOWS

2.1 Motivation

The effects of sand waves and/or ridges on hydrodynamics are usually overlooked in modeling studies considering basin-scale domains. In such cases, the friction coefficient is usually taken as an overall calibration parameter, thus taken constant in the entire domain (see Brakenhoff et al., 2020, and references therein). In order to better represent bedform-induced effects on basin-scale hydrodynamics, we hereby derive a parametrization of the bed shear stress, which incorporates local bedform field information. Therefore, by using the given parametrization on a basin-scale domain, the effects of bedforms can be accounted for, without actually resolving them.

2.2 Methodology

Consider a basin-scale domain (such as the North Sea, see Figure 3a), where different sand wave fields are present. Each sand wave field is characterized by the sand wave field profile $h(x,y)$, mean water depth H and orientation angle θ (defined as the angle of the crest-normal direction with respect to the x-coordinate). The momentum and continuity equations for a depth-averaged, shallow water flow on the f-plane read

$$\frac{\partial u}{\partial t} + u\frac{\partial u}{\partial x} + v\frac{\partial u}{\partial y} - fv + \frac{\tau_{b,x}}{H+h+\zeta} = -g\frac{\partial \zeta}{\partial x}\,, \tag{1a}$$

$$\frac{\partial v}{\partial t} + u\frac{\partial v}{\partial x} + v\frac{\partial v}{\partial y} + fu + \frac{\tau_{b,y}}{H+h+\zeta} = -g\frac{\partial \zeta}{\partial y}\,, \tag{1b}$$

$$\frac{\partial \zeta}{\partial t} + \frac{\partial}{\partial x}[(H+h+\zeta)u] + \frac{\partial}{\partial y}[(H+h+\zeta)v] = 0\,. \tag{1c}$$

Here, u and v are the depth-averaged velocities in the x and y directions, respectively. Furthermore, f is the Coriolis

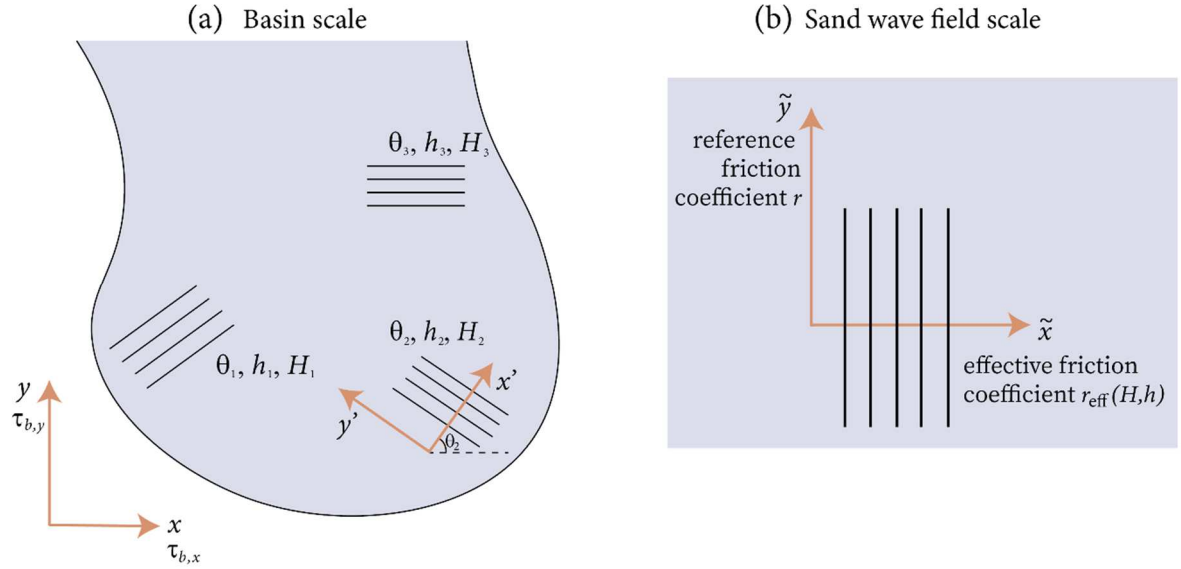

Figure 3. Sketch of the 2DH hydrodynamic model used: (a) basin-scale domain with several sand wave fields (each characterized by the bedform averaged orientation angle θ, sand wave field profile $h(x,y)$, and mean water depth H), and (b) sand wave field-scale domain with the $\tilde{x}$ axis pointing in the cross-crest direction. As a result of this choice of axis orientation, the friction experienced by the bedform-averaged flow is different in $\tilde{x}$ and $\tilde{y}$ directions. Note that two different reference systems are considered at basin scale, (x',y') being rotated with respect to (x,y).

parameter, g is the gravitational acceleration, and ζ is the vertical displacement of the sea surface with respect to the mean (defined at $z = 0$). The friction terms are written in terms of the bed shear stresses, $\tau_{b,x}$ and $\tau_{b,y}$. In the absence of bedforms ($h \equiv 0$), we adopt

$$\tau_{b,x} = ru, \quad \tau_{b,y} = rv, \tag{2}$$

where for convenience, as a first step, the bed shear stresses are parametrized to scale linearly with the flow velocities. Here, r is the *reference* friction coefficient, corresponding to a mean water depth H. The main motivation behind the following methodology is to obtain parametrizations for the bed shear stresses such that the dependence on bedforms is already accounted for in $\tau_{b,x}$ and $\tau_{b,y}$, and it is thus not explicitly included in the equations. We will see that due to the presence of sand waves, the expressions for the bed shear stresses will differ from those in Equation (2). As a result, $\tau_{b,x}$ and $\tau_{b,y}$ will depend on both flow velocity components u and v, and on sand wave field characteristics, such as bedform height, shape and angle of orientation.

We define three reference systems (Fig. 3): two basin-scale reference systems (x,y) and (x',y'), the latter being rotated by an angle θ with respect to the former. The third reference system, $(\tilde{x}, \tilde{y})$, is defined at sand wave field scale (also referred to as *local* reference system). The $\tilde{x}$-axis points in the cross-crest direction, and the $\tilde{y}$-axis int the along-crest direction.

By zooming in on the local reference system $(\tilde{x}, \tilde{y})$, we can assume periodicity in the $\tilde{x}$ direction and uniformity in $\tilde{y}$, because we consider regular bedforms (Fig. 3b). For simplicity, we assume steady flow and a low Froude number, such that the contribution of the free surface displacement to the local water depth can be neglected. We also decompose the forcing terms into two components,

$$-g\frac{\partial \zeta}{\partial \tilde{x}} = -\tilde{F} - g\frac{\partial \tilde{\zeta}}{\partial \tilde{x}}, \tag{3a}$$

$$-g\frac{\partial \zeta}{\partial \tilde{y}} = -\tilde{G}, \tag{3b}$$

where $\tilde{F}$ and $\tilde{G}$ are the components corresponding to the tidal wave, thus spatially uniform at sand wave field-scale. The corresponding momentum and continuity equations in the local reference system read

$$\tilde{u}\frac{\partial \tilde{u}}{\partial \tilde{x}} - f\tilde{v} + \frac{r\tilde{u}}{H+h} = -\tilde{F} - g\frac{\partial \tilde{\zeta}}{\partial \tilde{x}}, \tag{4a}$$

$$\tilde{u}\frac{\partial \tilde{v}}{\partial \tilde{x}} + f\tilde{u} + \frac{r\tilde{v}}{H+h} = -\tilde{G}, \tag{4b}$$

$$\frac{\partial}{\partial \tilde{x}}[(H+h)\tilde{u}] = 0. \tag{4c}$$

From Equation (4c), we infer a spatially uniform discharge $Q = (H+h)\tilde{u}$. Furthermore, we define the spatial averaging operator

$$\langle \cdot \rangle = \frac{1}{L}\int_0^L \cdot \, d\tilde{x}, \tag{5}$$

with L covering an integer number of bedforms. We also define sand wave field-averaged flows $\widetilde{U} = \langle \tilde{u} \rangle$ and $\tilde{V} = \langle \tilde{v} \rangle$, such that

$$\begin{aligned} \widetilde{U} = \langle \tilde{u} \rangle &= \left\langle \frac{Q}{H+h} \right\rangle = \frac{Q}{H}\left\langle \frac{1}{1+h/H} \right\rangle \\ &= \frac{Q}{H}\left\langle 1 - \frac{h}{H} + \frac{h^2}{H^2} - \cdots \right\rangle \\ &\approx \frac{Q}{H}\left(1 + \frac{\langle h^2 \rangle}{H^2}\right) = \frac{Q}{\alpha H}, \end{aligned} \tag{6}$$

thus $\tilde{u}$ can be written in terms of $\widetilde{U}$ as

$$\tilde{u} = \alpha \widetilde{U}\frac{H}{H+h}. \tag{7}$$

Here we have defined the factor α as

$$\alpha = \frac{H^2}{H^2 + \langle h^2 \rangle}. \tag{8}$$

Substituting Equation (7) into Equations (4a,b), and by taking the spatial average over the sand wave field, Equations (4a,b) reduce to

$$-f\tilde{V} + \frac{r_{\text{eff}}\widetilde{U}}{H} = -\tilde{F}, \tag{9a}$$

$$\alpha f \tilde{U} + \frac{r\tilde{V}}{H} = -\tilde{G}\,, \tag{9b}$$

respectively, where we have defined the *effective* friction coefficient r_{eff} as

$$r_{\text{eff}} = \alpha H^2 \left\langle \frac{1}{(H+h)^2} \right\rangle . \tag{10}$$

We thereby identify two different friction coefficients acting on the $\tilde{x}$ and $\tilde{y}$ directions (r_{eff} and r, respectively), with r_{eff} comprising sand wave-induced effects. Thus, sand wave-induced friction effects are experienced in the crest-normal direction.

By zooming out on the basin-scale and rotated reference system, (*x'*,*y'*) (Fig. 3a), we can include sand wave-induced effects on the basin-scale flow by considering the above obtained friction coefficient. Hence, sand wave information is already accounted for, and we do not need to explicitly include h in the momentum equations, yielding

$$\frac{\partial u'}{\partial t} + u'\frac{\partial u'}{\partial x'} + v'\frac{\partial u'}{\partial y'} - fv' + \alpha\frac{r_{\text{eff}}u'}{H+\zeta} = -g\frac{\partial \zeta}{\partial x'}\,, \tag{11a}$$

$$\frac{\partial v'}{\partial t} + u'\frac{\partial v'}{\partial x'} + v'\frac{\partial v'}{\partial y'} + \alpha f u' + \frac{rv'}{H+\zeta} = -g\frac{\partial \zeta}{\partial y'}\,. \tag{11b}$$

By transforming to the non-rotated basin-scale reference system, (*x*,*y*) (Fig. 3a), we obtain the depth-averaged, shallow water equations for a basin-scale, non-steady flow on the *f*-plane, in which the effects of bedforms are implicitly incorporated trough the bed shear stresses $\tau_{b,x}$ and $\tau_{b,y}$. As a result, the flow is not resolved at sand wave scale, yet the effects of bedforms on the flow are considered. The corresponding momentum equations read

$$\frac{\partial u}{\partial t} + u\frac{\partial u}{\partial x} + v\frac{\partial u}{\partial y} - fv + \frac{\tau_{b,x}}{H+\zeta} = -g\frac{\partial \zeta}{\partial x}\,, \tag{12a}$$

$$\frac{\partial v}{\partial t} + u\frac{\partial v}{\partial x} + v\frac{\partial v}{\partial y} + fu + \frac{\tau_{b,y}}{H+\zeta} = -g\frac{\partial \zeta}{\partial y}\,. \tag{12b}$$

Given that we are interested in the effects of bedform-induced friction, and for the sake of simplicity, α has been approximated to 1 in the Coriolis terms. Yet, it is included in the parametrization for r_{eff} (Eq. 10), on which $\tau_{b,x}$ and $\tau_{b,y}$ depend, i.e.,

$$\tau_{b,x} = u\frac{r_{\text{eff}}+r}{2} + \frac{r_{\text{eff}}-r}{2}(u\cos 2\theta + v\sin 2\theta) \tag{13a}$$

$$\tau_{b,y} = v\frac{r+r_{\text{eff}}}{2} + \frac{r_{\text{eff}}-r}{2}(u\,sin\,2\theta - v\,cos\,2\theta), \tag{13b}$$

which replaces Equation (2). Indeed, Equation (13) shows that both velocity components u and v affect both bed shear stress components. Note that the present analysis only considers hydrodynamics, so the bed is considered not to change over time.

2.3 Preliminary results

The described analysis has been applied in a local reference system with two different (synthetic) bedform patterns, both uniform in the $\tilde{y}$ direction, one purely sinusoidal and the other more sharply crested,

$$h_1(\tilde{x}) = \hat{h}\cos(k\tilde{x})\,, \tag{14a}$$

$$h_2(\tilde{x}) = \hat{h}\sum_{j=1}^{10}\frac{1}{j^2}\cos(jk\tilde{x}). \tag{14b}$$

Here k corresponds to the bedform wavenumber, $\hat{h}$ is the bedform amplitude, and we have taken a mean water depth of $H = 20$ m (Fig. 4a). Note that both bed profiles have the same mean water depth.

The respective values of r_{eff} increase with the bedform amplitude relative to the mean water depth (Fig. 4b), with r_{eff} being always larger than r. Furthermore, the sinusoidal sand wave

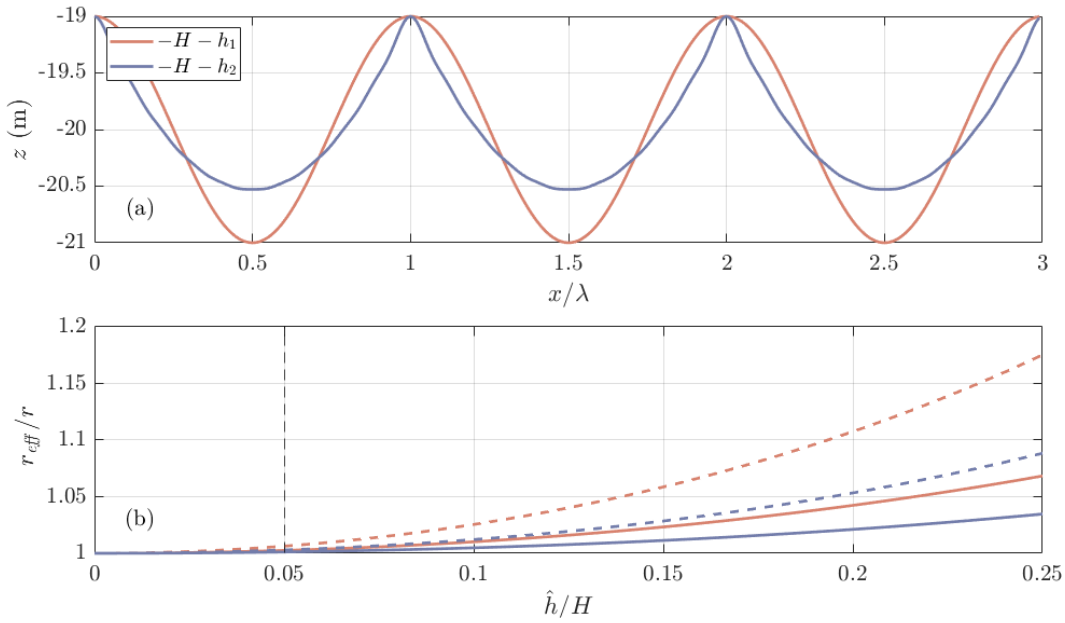

Figure 4. (a) Different sand wave profiles used in the present study, and (b) resulting effective friction coefficient r_{eff} relative to the reference friction coefficient r for different sand wave field amplitudes. Thick solid lines in panel (b) correspond to the situation in which the bed shear stress is parametrized linearly on the flow velocity, while thick dashed lines correspond to a bed shear stress scaling quadratically on the flow velocities (further discussed in §2.4.1). The vertical dashed line in panel (b) corresponds to the situation depicted in panel (a), where the sand wave field amplitude is 1 m. We have taken a Coriolis parameter representative for the North Sea ($f = 1.15 \cdot 10^{-4}$ s^{-1}), and a linear friction coefficient of $r = 2.5 \cdot 10^{-3}$ m/s.

field results in a higher friction coefficient (for equal sand wave field amplitudes). This is because the region over which the bedform is above mean water depth is larger in the sinusoidal bedform case, thus resulting in higher friction. Note that the results are independent on the chosen bedform wavelength.

2.4 Discussion

2.4.1 Flow deflection over a wavy bed

Starting from Equation (9) and further considering the situation in which the same forcing is present, but now on a flat bed, we can obtain the flow on a wavy bed (U,V) with respect to that on a flat bed (U_0,V_0),

$$U = \frac{r^2 H^{-2} + f^2}{r_{\text{eff}} r H^{-2} + \alpha f^2} U_0 \,, \qquad (15a)$$

$$V = V_0 + \frac{f}{H} \frac{r_{\text{eff}} - \alpha r}{r_{\text{eff}} r H^{-2} + \alpha f^2} U_0 \,. \qquad (15b)$$

This results in variations in flow magnitude and angle (Fig. 5). These effects depend, however, on the angle ϕ_0 of the flow with respect to the $\tilde{x}$ axis. When the flow is purely in the $\tilde{y}$ direction ($\phi_0 = \pm 90°$) the flow is not modified because the sand waves are straight-crested in this direction.

2.4.2 Simplifications

Several simplifications have been made in order to obtain the sand wave field-scale friction parametrizations. Most importantly, the bed shear stress has been taken to scale linearly on the flow velocities, whereas it is usually taken to scale quadratically (Soulsby, 1997). The effects of bedforms become more relevant if the bed shear stress is taken to scale quadratically on the flow velocity (dashed lines in Figure 4b). Future work will incorporate this formulation in order to better capture the effects of bedforms on friction.

Separately, for simplicity we have also assumed steady state and low Froude number when computing the parametrizations at sand

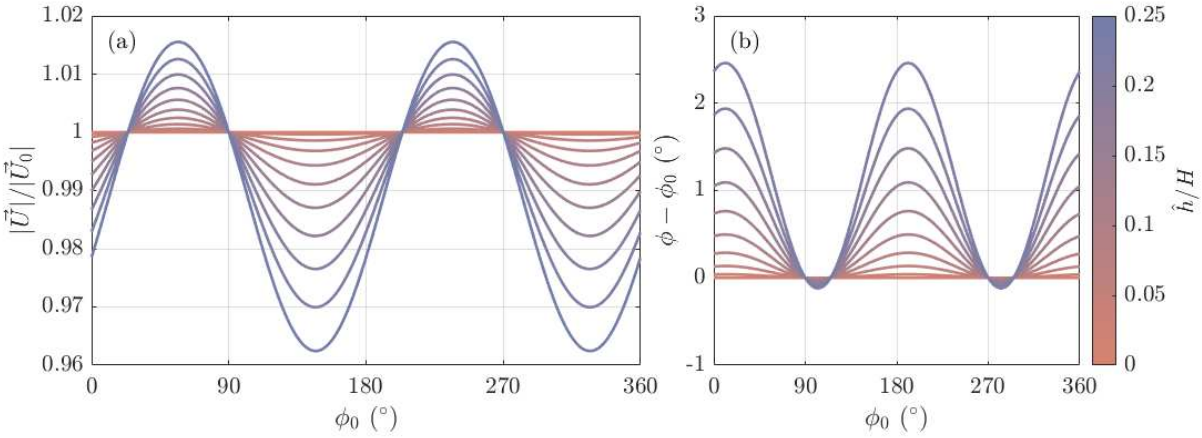

Figure 5. Effects of sand wave-induced friction on local flow (sand wave-scale) depending on the sand wave amplitude with respect to the mean water depth, and the flow angle with respect to the $\tilde{x}$ axis. There are variations in flow magnitude (a), and angle (b). The applied sand wave field is sinusoidal (Eq. 12a).

wave field scale (Eq. 4), but we aim to use them in non-steady models, which do not necessarily lie in the low Froude number regime (Eq. 10).

3 CONCLUSIONS AND FUTURE WORK

We have developed friction coefficient parametrizations that serve to include the effects of sand waves on basin-scale modeling studies. The presented results show variations in flow magnitude and angle due to the presence of bedforms. The magnitude of these effects depends on the bedform amplitude with respect to the mean water depth, and on the flow angle with respect to the sand wave field orientation.

The model presented will be further developed. Most importantly, the bed shear stresses should be taken quadratic on the flow velocities. Furthermore, the overall effect of different (and realistic) sand wave fields on a basin-scale flow will be tested in the future.

4 ACKNOWLEDGEMENTS

This work is part of the MELODY project, which is partly funded by NWO (Dutch Research Council).

5 REFERENCES

Blondeaux, P., 1990. Sand ripples under sea waves Part 1. Ripple formation. Journal of Fluid Mechanics, 218, 1-17. doi:10.1017/S0022112090000908

Brakenhoff, L., Schrijvershof, R., van der Werf, J., Grasmeijer, B., Ruessink, G., & van der Vegt, M., 2020. From ripples to large-scale sand transport: the effects of bedform-related roughness on hydrodynamics and sediment transport patterns in Delft3D. Journal of Marine Science and Engineering, 8(11), 892. doi:10.3390/jmse8110892

Hulscher, S.J.M.H., 1996. Tidal-induced large-scale regular bed form patterns in a three-dimensional shallow water model. Journal of Geophysical Research: Oceans, 101(C9), 20727-20744. doi:10.1029/96JC01662

Roos, P.C., Hulscher, S.J.M.H., Knaapen, M.A.F., & van Damme, R.M.J., 2004. The cross-sectional shape of tidal sandbanks: Modeling and observations. Journal of Geophysical Research: Earth Surface, 109(F2). doi:10.1029/2003JF000070

Soulsby, R.L., 1983. The Bottom Boundary Layer of Shelf Seas, in Elsevier Oceanography Series. Elsevier, 189-266

Soulsby, R.L., 1997. Dynamics of marine sands. T. Telford London, UK.

van der Spek, A., van der Werf, J., Oost, A., Vermaas, T., Grasmeijer, B., & Schrijvershof, R. 2022. The lower shoreface of the Dutch coast – An overview. Ocean & Coastal Management. doi:10.1016/j.ocecoaman.2022.106367